



Poly(butylene adipate-co-terephthalate) biodegradation by *Purpureocillium lilacinum* strain BA1S

Wei-Sung Tseng¹ · Min-Jia Lee¹ · Jin-An Wu² · Shin-Liang Kuo² · Sheng-Lung Chang² · Shu-Juan Huang² · Chi-Te Liu^{1,3,4}

Received: 15 May 2023 / Revised: 18 July 2023 / Accepted: 21 July 2023 / Published online: 1 August 2023
© The Author(s), under exclusive licence to Springer-Verlag GmbH Germany, part of Springer Nature 2023

Abstract

Poly(butylene adipate-co-terephthalate) (PBAT), a promising biodegradable aliphatic-aromatic copolyester material, can be applied as an alternative material to reduce the adverse effects of conventional plastics. However, the degradation of PBAT plastics in soil is time-consuming, and effective PBAT-degrading microorganisms have rarely been reported. In this study, the biodegradation properties of PBAT by an elite fungal strain and related mechanisms were elucidated. Four PBAT-degrading fungal strains were isolated from farmland soils, and *Purpureocillium lilacinum* strain BA1S showed a prominent degradation rate. It decomposed approximately 15 wt.% of the PBAT films 30 days after inoculation. Scanning electron microscopy (SEM), Fourier transform infrared spectroscopy (FTIR), and Liquid chromatography mass spectrometry (LC–MS) were conducted to analyze the physicochemical properties and composition of the byproducts after biodegradation. In the presence of PBAT, the lipolytic enzyme activities of BA1S were remarkably induced, and its cutinase gene was also significantly upregulated. Of note, the utilization of PBAT in BA1S cells was closely correlated with intracellular cytochrome P450 (CYP) monooxygenase. Furthermore, CreA-mediated carbon catabolite repression was confirmed to be involved in regulating PBAT-degrading hydrolases and affected the degradation efficiency. This study provides new insight into the degradation of PBAT by elite fungal strains and increases knowledge on the mechanism, which can be applied to control the biodegradability of PBAT films in the future.

Key points

- *Purpureocillium lilacinum* strain BA1S was isolated from farmland soils and degraded PBAT plastic films at a prominent rate.
- The lipolytic enzyme activities of strain BA1S were induced during coculture with PBAT, and the cutinase gene was significantly upregulated during PBAT degradation.
- CreA-mediated carbon catabolite repression of BA1S plays an essential role in regulating the expression of PBAT-degrading hydrolases.

Keywords PBAT plastic · Lipolytic enzymes · Cutinase · Cytochrome P450 · Carbon catabolite repression · *Purpureocillium lilacinum*

Introduction

Poly(butylene adipate-co-terephthalate) (PBAT) is an aliphatic and aromatic copolyester that is synthesized by a polycondensation reaction of 1,4-butanediol (BDO), adipic acid (AA), and terephthalic acid (PTA) (Jian et al. 2020). PBAT is a promising biodegradable material that shows similar mechanical properties to low-density polyethylene (LDPE) and is more flexible than most biodegradable polyesters,

such as PLA and PBS (Bordes et al. 2009; Nagarajan et al. 2013). PBAT-based products exhibit good hydrophilicity, excellent mechanical properties, and biodegradability and are widely used in many applications, such as packaging, mulch film, and cutlery (Kargarzadeh et al. 2020). Various aliphatic and aromatic oligomers could be determined and identified during PBAT degradation, but only the monomers BDO, AA, and PTA were observed at the end of the experiments (Witt et al. 2001). The rate of PBAT biodegradation is very low under mesophilic conditions (Rychter et al. 2010; Šerá et al. 2016) but is rapid at relatively high temperatures

Extended author information available on the last page of the article

(50–60 °C) in composts (Saadi et al. 2013; Svoboda et al. 2019).

The common plastic-degrading enzymes are carboxylic ester hydrolases (EC 3.1.1), which are often annotated as lipases, esterases, cutinases, amidases, or proteases; these hydrolases catalyze the depolymerization of polymer chains into simpler monomeric units (Ali et al. 2021; Buchholz et al. 2022; Kaushal et al. 2021). Fragments of polymeric materials can be used directly by microorganisms or indirectly through metabolic intermediates as sources of nutrients or energy for growth and reproduction (Krzan et al. 2006). Intracellular cytochrome P450 (CYP) enzymes, the ubiquitous superfamily of monooxygenases, play an essential role in the assimilation of nonactivated hydrocarbons (aliphatic, alicyclic, and aromatic molecules) from lipophilic compounds to more hydrophilic derivatives through intricate processing (Črešnar and Petrič 2011; Yeom et al. 2021). The monooxygenase activity of intracellular cytochrome P450 (CYP) is an essential index for plastic degradation (Ali et al. 2021). It has been reported that P450 monooxygenases are involved in the cleavage of saturated carbon–carbon bonds during the biodegradation of PE and PS (Matthews et al. 2017; Xu et al. 2019). NADPH-cytochrome P450 reductase (CPR) is an essential enzyme for electron transfer in the cytochrome P450 system, and its activity can usually represent that of CYP (Jing et al. 2018).

Purpureocillium lilacinum (formerly *Paecilomyces lilacinus*) is a species of filamentous and entomopathogenic fungus and is among the most promising and practicable biocontrol agents against plant parasite nematodes (Sarven et al. 2019; Yang et al. 2015). This fungal species has been reported to biodegrade a variety of petroleum hydrocarbons (Benguenab and Chibani 2021), such as the synthetic plastics PBAT, PLA, LDPE, PBSA, and PU (Lee et al. 2021; Spina et al. 2021; Tan et al. 2008; Yamamoto-Tamura et al. 2015).

In this study, we screened and isolated several PBAT-degrading isolates from farmland soils and identified a potential fungal strain BA1S of *P. lilacinum*. We aim to improve and control PBAT biodegradability by elucidating the biodegradation properties and related mechanisms of this strain.

Materials and methods

Plastic materials

Poly(butylene adipate-co-terephthalate) (PBAT) particles and films were provided by the Material and Chemical Research Laboratories of the Industrial Technology Research Institute (ITRI). The number-average molecular weight (Mn) and the average molecular weight (Mw) of the

PBAT films were 7732 and 58919 g/mol, respectively. The molar ratio of the butylene adipate (BA) unit to the butylene terephthalate (BT) unit in the copolymer PBAT was 0.52/0.48 mol_{BA}/mol_{BT}, which was determined by ¹H NMR spectroscopy in CDCl₃.

Soil sampling locations

Soil samples (9 samples in total) were collected from the topsoil (5–20 cm depth) at the following sites in Taiwan. Three samples were collected in New Taipei City (Danshui mangrove wetland soil, 25°09'30.1"N 121°27'22.5"E) and Taipei City (National Taiwan University field soil, 25°00'56.0"N 121°32'22.9"E, and compost soil, 25°00'57.9"N 121°32'31.4"E). Three samples were collected in Miaoli County (strawberry soil, 24°26'45.3"N 120°52'51.3"E; cabbage and tomato soils, 24°27'39.8"N 120°43'08.7"E); one sample was collected in Chiayi County (banana soil, 23°27'27.6"N 120°25'30.5"E); two samples were collected in Tainan City (beach soil, 22°58'49.8"N 120°09'15.2"E; field soil, 23°08'32.8"N 120°08'24.0"E).

Screening and isolation of PBAT-degrading microorganisms

The screening system was based on a modified clear zone method (Chien et al. 2022) to prepare the PBAT emulsified plates. In this method, 100 µL of the soil suspension (prepared by dissolving 1 g of soil sample in 5 mL of distilled water and shaking at 100 rpm for 30 min at room temperature) was spread over the surface of the emulsified PBAT agar plate with glass beads, and the plates were incubated at 25 °C and 30 °C. The streaking plate method was used to isolate pure cultured PBAT-degrading microorganisms that had formed clear zones on the plates. A modified method was used by directly adding the soil suspension into the holes (created by the tail base site of a 200-µL microtip) on the PBAT plate and then cultivating the plates in the incubator until clear zones formed. To isolate PBAT-degrading bacteria, we applied the antifungal agent nystatin (0.5 mg/ml in DMSO) to inhibit the growth of fungi (Atiq et al. 2010).

Identification and phylogenetic analysis of microbial isolates

The total genomic DNA (gDNA) of the isolates was extracted by the Presto™ Mini gDNA kit (Geneaid Biotech Ltd., Taipei, Taiwan). Fungal DNA used primers ITS5 (5'-GGAAGTAAAAGTCGTAACAAGG-3') and ITS4 (5'-TCC TCCGCTTATTGATATGC-3') to amplify the internal transcribed spacer (ITS) and 5.8S rRNA between 18S rRNA and 28 rRNA regions (Gardes and Bruns 1993; Ragonezi et al. 2013). Amplicons were compared with the NCBI GenBank

database, and the species were identified using the Basic Local Alignment Search Tool (BLAST) (<https://blast.ncbi.nlm.nih.gov/Blast.cgi/>) after Sanger sequencing. The phylogenetic tree was generated using Molecular Evolutionary Genetics Analysis (MEGA) software version X (<https://www.megasoftware.net/>) with the neighbor-joining method (1,000 bootstrap repeats). The strain *P. lilacinum* BA1S was deposited in the Bioresource Collection and Research Center (BCRC, <https://www.bcrc.firdi.org.tw/en/home/>) under accession number BCRC FU31904. The ITS sequence of *Purpureocillium lilacinum* BA1S was submitted to the GenBank database under accession number OQ781167.

Growth media and culture conditions for the isolates

The fungal strains were initially cultured on potato dextrose agar (PDA) plates at 30 °C for 7–10 days until spores were generated. The spores were collected with sterile distilled water containing 0.05% Tween 20 (Bioman Scientific Co., Ltd., Taipei, Taiwan). The procedure for mycelia preparation was performed following a previous method (Xia et al. 2019) with some modifications.

Determination of microbial PBAT biodegradability

To determine the PBAT decomposing ability of different strains, microbes were cocultured with PBAT films in a carbon-free broth. Ten pieces of PBAT plastic films (size: 2.5 cm × 5 cm, thickness: 30 μm) were sterilized with 6% sodium hypochlorite and 75% ethanol for 30 min and placed into 100 mL of the broth after washing with sterile water. One hundred microliters of every 10⁸ spores/mL spore solution or 10⁸ CFU/mL bacterial broth was added into the broth for different tests (equivalent to 10⁶ spores/mL or 10⁶ CFU/mL). Three pieces of plastic film were collected for each sampling. The attached microbes were gently removed by washing them with a commercial detergent (PAOS®, Nice Co., Taiwan), and the plastics were dried in a 60 °C oven. The degradation rate of the PBAT films was calculated using the following modified equation (Jia et al. 2021a):

$$\text{Degradation rate of the PBAT films (\%)} = (W_0 - W_t) / W_0 \times 100\%,$$

where W_0 is the weight of the PBAT films before degradation and W_t is the weight after the incubation time.

SEM analysis

To confirm the microbial adhesion and the surface morphology of the plastic film during degradation, the sample was evaluated by scanning electron microscopy (SEM) (Jeol, JSM-6510, Tokyo, Japan) as described by (Yoshida et al. 2016).

FTIR analysis

Fourier transform infrared spectroscopy has been used in various studies to investigate the biodegradation of plastics and analyze the structural changes in polymers (Han et al. 2021; Kilic et al. 2019; Shah et al. 2008). The PBAT films were washed by DDW to remove the attached microbes and were scanned in a wavelength range of 400–4000 cm⁻¹ by an attenuated total reflection Fourier transform infrared spectrometer (ATR-FTIR; Thermo Scientific Nicolet 380).

LC–MS analysis

We used the Rapid Separation LC (RSLC) system (Thermo Scientific, Dionex serial No. 8054164) with a quadrupole time-of-flight (QTOF) mass spectrometer (Bruker serial No. 282001-00040) to evaluate the remaining plastic residues of the PBAT films in the broth after degradation by *P. lilacinum* BA1S for 14 days. The experimental conditions followed those in previous studies (Jia et al. 2021a; Sato et al. 2017). The mobile phase used was water-methanol. The chemical compounds were unambiguously confirmed by the standards based on the retention time (RT), ultraviolet spectra (UV), and mass spectrometry (MS) results.

Extracellular lipolytic enzyme assay

To concentrate the extracellular crude protein secreted by the individual isolates, we used the diafiltration method and dialysis in 50 mM NaH₂PO₄ buffer (pH 7.0). Lipolytic enzyme activity was spectrophotometrically determined by the colorimetric method using varying acyl chain lengths of *p*-nitrophenyl esters (Gilham and Lehner 2005; Hwang et al. 2005). All procedures were modified according to a previous study (Chien et al. 2022).

Cytochrome P450 reductase activity assay

P. lilacinum BA1S was cultured with PBAT films in carbon-free minimal broth for 7, 14, and 21 days. Potato dextrose broth (PDB) (Bioman Scientific Co., Ltd) and carbon-free minimal broth with 1% glucose (Bioman Scientific Co., Ltd) were used as the control treatments (incubated for 5–7 days). The separated mycelium was washed twice with 1 × PBS buffer and ground into powder by homogenizing with glass beads using Tissue Lyser II (Qiagen, USA). Intracellular protein was extracted by adding extraction buffer (50 mM K₂HPO₄, 5 mM MgCl₂, 5 mM 2-mercaptoethanol, and 0.5 mM EDTA) (Battaglia et al. 2011) and then shaking for 1 h at 4 °C. After that, the mixtures were centrifuged for 10 min at 12,000 rpm at 4 °C, and the supernatant was filtered through a 0.22 μm filter. The extracted protein concentration was quantified by the Bradford method with bovine serum albumin (BSA) as

a standard. The NADPH cytochrome P450 reductase activity assay was measured based on the reduction activity of the surrogate electron acceptor cytochrome c (Guengerich et al. 2009; Huang et al. 2015).

Gene expression analysis of *P. lilacinum* by quantitative real-time PCR (qPCR)

P. lilacinum BA1S was cocultured with PBAT film, which was the sole carbon source. On the other hand, 1% glucose (Biomax Scientific Co., Ltd) was used as a control carbon source for *P. lilacinum* BA1S incubation for 5–7 days. The mycelium was gently separated from the surface of PBAT plastic films, quickly frozen in liquid nitrogen, and stored at -80 °C in TRIzol® reagent (Invitrogen, USA) for RNA extraction with a Direct-zol™ RNA MiniPrep kit (Zymo Research, USA) following the manufacturer's instructions. Total RNA was treated with a TURBO DNA-free™ Kit (Invitrogen, USA), and first-strand cDNA was synthesized by SuperScrip™ IV Reverse Transcriptase (Invitrogen, USA) with oligo (dT)₂₀ primers. Real-time quantitative PCR analyses of gene expression were performed with a LightCycler 480 System (Roche Diagnostics, Germany) using LightCycler 480 SYBR Green I Master Mix (Roche Diagnostics, Germany). For all qPCRs, two technical replicates were run for each biological replicate. The housekeeping actin gene was used for transcript normalization as the reference gene (Wang et al. 2016). Relative expression (fold change) of target genes was calculated by the $2^{-\Delta\Delta CT}$ method (Livak and Schmittgen 2001), and the primer efficiency was determined using standard curves with five 1:10 dilutions of cDNA (Pfaffl 2001). The associative genes chosen to evaluate the correlation with PBAT degradation are listed in Table S1.

Statistical analysis

All statistical analyses of variance were performed by one-way ANOVA using R version 4.1.0. Tukey's honestly significant difference (Tukey's HSD) test was used for multiple comparisons among testing groups. Student's t test was applied to determine the difference between the means of two groups. Groups were considered statistically significant when $p < 0.05$.

Results

Screening and identification of potential PBAT-degrading strains

We isolated several potential fungal strains from the respective transparent clearing zones on the plates by serial dilution and the streaking plate method (data not shown). In the first screening, BA1S, BA2S, CB1S, and SB1S were selected

as potential PBAT degraders, and their biodegradabilities were further verified by inoculating them on emulsified PBAT agar plates (Fig. 1A). BA1S and BA2S were isolated from the banana field located in Chiayi County, and CB1S and SB1S were isolated from the cabbage field and strawberry field located in Miaoli County, respectively. According to the morphological characteristics of the isolates with hyphae and spores on the PDA plates, we assumed that these four isolates (BA1S, BA2S, CB1S, and SB1S) were fungi (Fig. 1A). They were identified by phylogenetic analysis of partial sequences of ITS genes (including the 5.8S ribosomal RNA gene), which showed high sequence similarity with *Purpureocillium lilacinum* (100%), *Penicillium citrinum* (100%), *Aspergillus fumigatus* (100%), and *Westerdykella dispersa* (100%). Additionally, a phylogenetic tree was built based on the ITS sequences of the isolates, and the reference strains were used to elucidate their taxonomic relationship (Fig. 1B).

P. lilacinum BA1S showed a good ability to adhere and degrade PBAT films

For the sample inoculated with *P. lilacinum* BA1S, the surface of the whole film was covered by a compact layer of mycelia. In contrast, those inoculated with the other fungal strains (i.e., BA2S, CB1S, and SB1S) were covered with a thin layer of mycelia on the surface. After the superficial mycelia were removed, the whole surface of the plastic film inoculated with *P. lilacinum* BA1S was evenly opaque, while the other treatments displayed unevenly transparent places on the surfaces of the films (Fig. 2A). Although the difference in appearance between the PBAT films with higher degradation and those with lower degradation seemed insignificant, we observed that as the degradation level increased, the opacity of the films also increased. The degradation rates of individual isolates were determined by the weight loss of the respective films. After 60 days of incubation, the PBAT degradation rates of *P. lilacinum* BA1S, *P. citrinum* BA2S, *A. fumigatus* CB1S, and *W. dispersa* SB1S were 15.27%, 5.35%, 7.89%, and 4.04%, respectively (Fig. 2B). Accordingly, *P. lilacinum* strain BA1S was chosen for further experiments.

Surface appearance of PBAT films degraded by *P. lilacinum* BA1S

SEM analysis was conducted to observe the morphological change in the PBAT film surface degraded by *P. lilacinum* BA1S after 14 days of incubation. As shown in Fig. S3A, the untreated BA1S film displayed a smooth surface. On the other hand, many cracks and roughness were observed on the BA1S-treated film surface (Fig. 3A). The inoculated spores attached to the

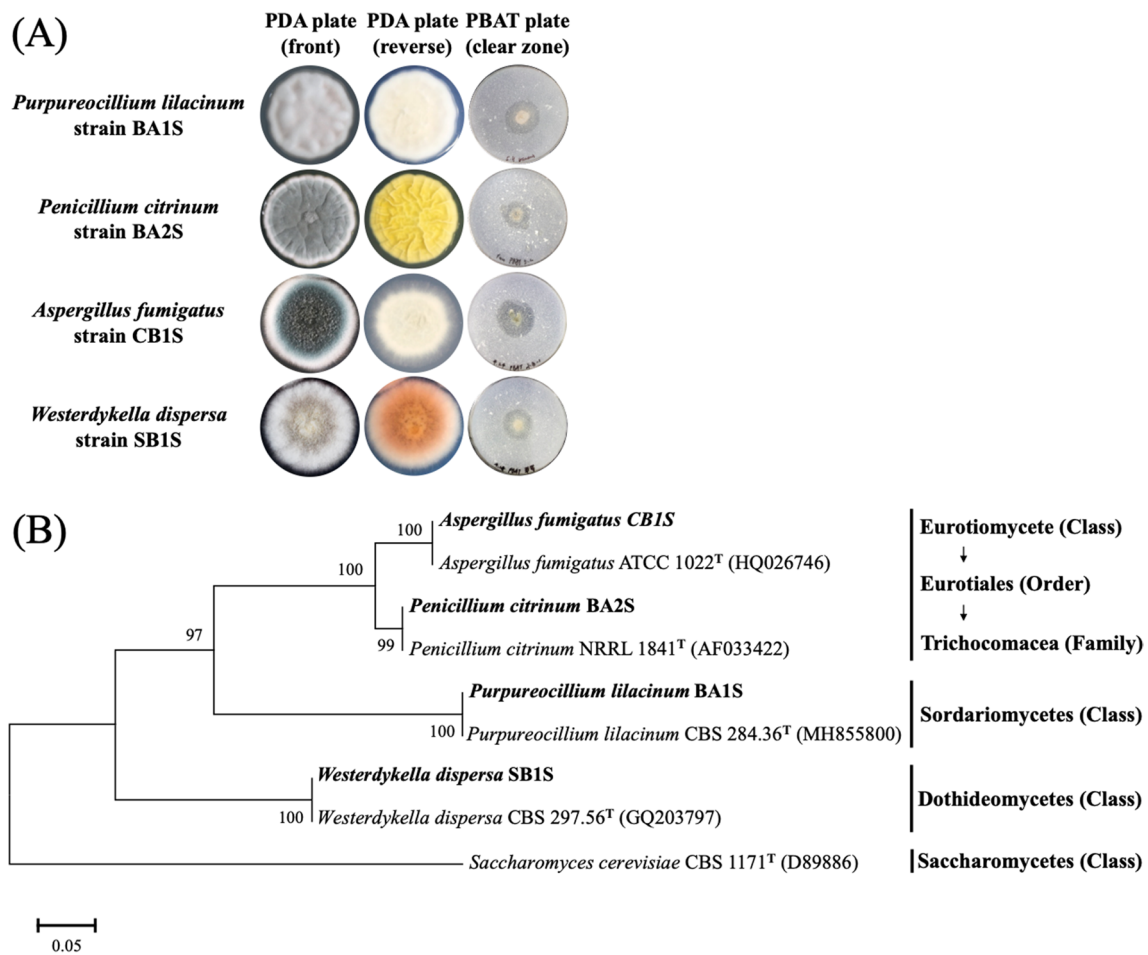


Fig. 1 Morphologies and phylogenetic tree of the potential PBAT-degrading fungal strains isolated from farmlands. **A** Potato dextrose agar (PDA) plates were used to cultivate the fungal isolates. Spores and mycelia with different morphologies were observed on the surface of the plates. The right-most panel indicates that the PBAT biodegradabilities of individual strains were evaluated by the sizes of transparent clearing zones on the emulsified PBAT plates. **B** ITS gene-based phylogenetic affiliation of the PBAT-degrading isolates. A phylogenetic tree was constructed from a comparison of the 5.8S

ribosomal RNA gene and the partial sequences of the internal transcribed spacer (ITS) region using neighbor-joining analysis of a distance matrix with Kimura’s two-parameter model. The pattern of branching was based on the class of different strains. Bootstrap values (expressed as percentages of 1000 replications) of more than 75% are shown at the nodes. The scale bar represents 0.05 substitutions per nucleotide position. Type strains for each species are designated with a superscript T, and *Saccharomyces cerevisiae* CBS 1171 was used as an outgroup

surface of the film (Fig. 3B, arrow) germinated into hyphae, and then the mycelia spanned the film surface (Fig. S1B). Additionally, a specialized appressorium structure of the strain was adhered on the surface (Fig. 3C, arrow). Moreover, various spherical structures were found on the degraded surface, and tangled hyphae were embedded in their surroundings (Figs. 3D and S1C). The hyphae also penetrated into the interior of the spherical structures (Figs. 3E, F, and S1D). The broken and hollow spherical structures (Fig. S1E) indicate that the composition of the film was degraded by the fungal strain (Fig. S1F).

Structural changes and degradation products of the PBAT films degraded by *P. lilacinum* BA1S

FTIR analysis was performed to confirm the components of the functional groups of the PBAT films before and after degradation (14 dpi). Referring to the peak positions for individual functional groups in the previous literature (Kilic et al. 2019), the peaks for C-H stretching in aliphatic and aromatic portions of functional groups were identified at 3011–2855 cm⁻¹ and 1710 cm⁻¹ (C=O stretching in ester bond), respectively (Fig. S2). The other peaks were also recognized at 1255 cm⁻¹ (C-O twisting in ester bond), 726 cm⁻¹

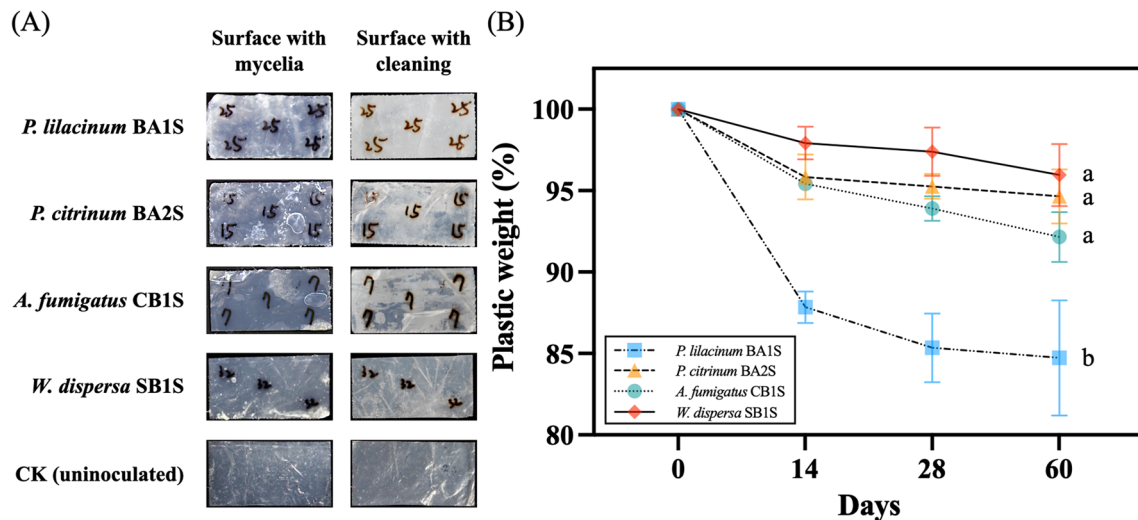


Fig. 2 Colonization of the isolates on the surface of PBAT films and their degradation abilities. Four fungal isolates were cocultured with ten pieces of PBAT plastic films (size: 2.5 cm × 5 cm, thickness: 30 μm) at 30 °C in carbon-free medium. **A** Plastic films were collected 28 days after incubation (DPI). The attachment of the mycelia was shown on the film surface (“Surface with mycelia”), and traces

of decomposition were observed after removing the attached mycelia with DDW (“Surface with cleaning”). **B** Plastic films were sampled at 0, 14, 28, and 60 DPI. Weight loss was measured and calculated after surface cleaning and drying. The values are expressed as the mean ± standard deviation ($p < 0.05$; Tukey’s post hoc ANOVA)

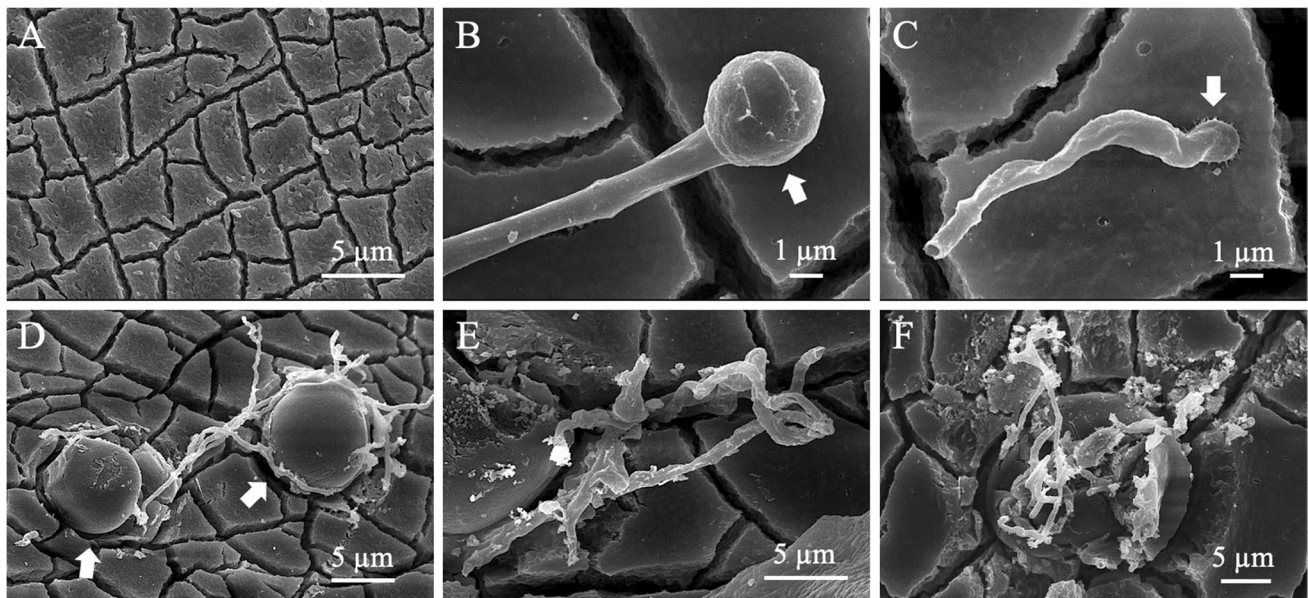


Fig. 3 Scanning electron microscopy images of PBAT film partially degraded by *P. lilacinum* BA1S after 14 days. **A** BA1S-treated film. **B** Spore (arrow) and the germinated mycelia. **C** The specialized struc-

ture is the appressorium (arrow). **D** Spherical structures formed during degradation. **E, F** The tangled hyphae were embedded in the surrounding spherical structure

(4 adjacent CH₂ groups stretching), and 901–700 cm⁻¹ (benzene bending). All absorption spectra of the degraded PBAT films were decreased in comparison with those before degradation, suggesting that the films underwent degradation. Among the peaks, those at 1710 cm⁻¹ (C=O) and

1255 cm⁻¹ (C-O) were markedly reduced, suggesting that the ester bonds underwent hydrolytic cleavage.

To identify the products of the PBAT film that remained after degradation by *P. lilacinum* BA1S for 14 days, we analyzed the composition of the filtered culture medium by

LC–MS. As shown in Fig. S3, two terephthalate derivatives of the PBAT monomer were identified. The expected molecular weights of the extracted chemicals were 166.03 ($C_8H_6O_4$) and 149.02 ($C_8H_6O_3^-$) g/mol, respectively. This

suggests that these terephthalate derivatives were the residue of degradation products.

Extracellular and intracellular enzyme activities of *P. lilacinum* BA1S induced by PBAT

To assess the activities of the extracellular lipolytic enzymes and intracellular CPR enzymes induced by PBAT in the culture medium, the crude proteins of *P. lilacinum* BA1S were collected from individual treatments cultured with PBAT films for two weeks. The CK group indicates that *P. lilacinum* BA1S was cultured in 1% glucose medium for 5 days. The extracellular lipolytic enzyme activities against short-chain to long-chain fatty acids were all increased after being cultured with PBAT films (Fig. 4), especially for the catalyzed C4, C8, C10, and C12 substrates.

As shown in Fig. 5A, the PBAT-induced protein increased the absorbance peaks at 520 and 550 nm, and the denatured protein demonstrated spectral similarity to the control (without protein), suggesting that the reduction originated from the contribution of the CPR enzyme. In addition, the CPR activities of the controls (PDB medium and carbon-free basal medium with 1% glucose) were 0.0028 and 0.0043 nmol/min/ng, respectively, while the enzyme activities were 0.0057, 0.006, and 0.0067 nmol/min/ng after being cultured with PBAT for 7, 14, and 21 days (Fig. 5B). Accordingly, the cytochrome P450 reductase activity of *P. lilacinum* BA1S was enhanced by the PBAT film, and

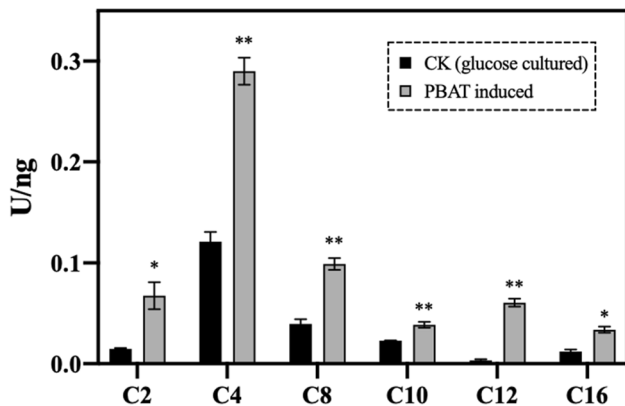


Fig. 4 Extracellular lipolytic enzyme activities of *P. lilacinum* BA1S in the presence of PBAT films. Extracellular crude proteins were concentrated from the culture medium supplemented with 1% glucose and PBAT films. The lipolytic enzyme activities of *P. lilacinum* BA1S were determined by chromogenic substrates (i.e., *p*-nitrophenyl esters with different chain lengths). The enzyme activity was defined as the amount of the released 1 μ mol *p*-nitrophenol per minute (U) in one unit of the crude protein (ng). The results are presented as the mean \pm standard deviation (*N.S.: $p > 0.05$, *: $p < 0.05$, **: $p < 0.01$; Student’s t-test)

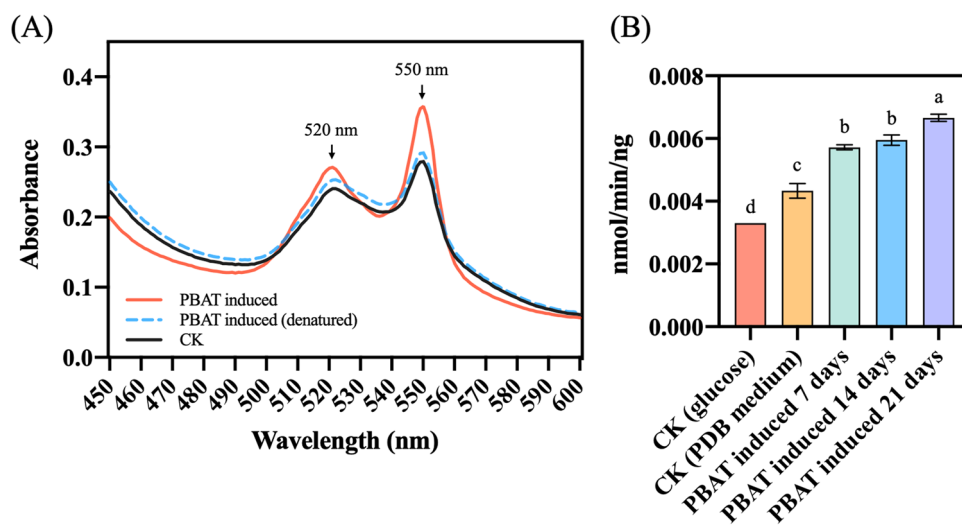


Fig. 5 Cytochrome P450 reductase activity of *P. lilacinum* BA1S induced by PBAT film. Intracellular proteins of BA1S were extracted and reacted with horse cytochrome c to measure cytochrome P450 reductase activity. **A** The absorbance spectra of cytochrome c from 450–600 nm were detected after reacting for 1 h. The red color represents the strain that was cocultured with PBAT for 14 days. The blue dashed line represents the extracted protein that was denatured by heating. CK (black color) used the extraction buffer as a control.

B Comparison of the cytochrome P450 reductase activities induced by PBAT for 7, 14, and 21 days. The control trials were extracted from mycelia cultured in PDB medium and carbon-free medium with 1% glucose. The activity was defined as the amount of the reduction of cytochrome c (nmol) per minute in one unit of the extracted protein (ng). The values of each treatment were expressed as the mean \pm standard deviation ($p < 0.05$; Tukey’s post hoc ANOVA)

the enzyme activity was increased during incubation with PBAT.

Gene expression of *P. lilacinum* BA1S during the early stages of PBAT biodegradation

To evaluate the expression of the related genes during the early stages of degradation, *P. lilacinum* BA1S was cocultured with PBAT films for less than 3 days and compared with those without PBAT addition. We extracted the total RNA of the initially germinated spores (Fig. 6Ab) at 16 h and 3 days. The expression of the ungerminated spores in the respective treatments (Fig. 6Aa) was used as a reference for the analyses (i.e., as an initial value). As shown in Figs. 6Ac and Ad, no significant difference in the morphology and amounts of germinated spores of *P. lilacinum* BA1S was observed between the treatments with and without PBAT. The log₂-fold change values (Fig. 6B and Table S2) and the relative expression (Fig. 6C) of the cutinase gene depicted were significantly upregulated when cultured with PBAT after 16 h and 3 days of incubation. In contrast, those for the treatments in the carbon-free basal medium without PBAT

addition were downregulated. On the other hand, the expression of the carbon catabolite repression-related gene (*CreA*) was significantly downregulated for the treatments cultured with PBAT, but the treatments in the carbon-free medium were significantly downregulated at 16 h and upregulated at 3 days (Fig. 6B).

Gene expression of *P. lilacinum* BA1S with long-term incubation of PBAT biodegradation

To elucidate the expression of the target genes and examine the correlation to PBAT biodegradation, we analyzed the transcripts of the treatments with and without PBAT for long-term incubation (16 h to 30 days). Glucose was chosen as the carbon control for comparison to PBAT. As shown in Fig. 7 and Table S3, the log₂-fold change values of the cutinase and cytochrome P450 genes were significantly upregulated after being cultured with PBAT film. In contrast, those of the cAMP receptor and cytochrome P450 reductase (CPR) were significantly downregulated during incubation. On the other hand, the subtilisin (peptidase) gene was significantly upregulated in the early stages of

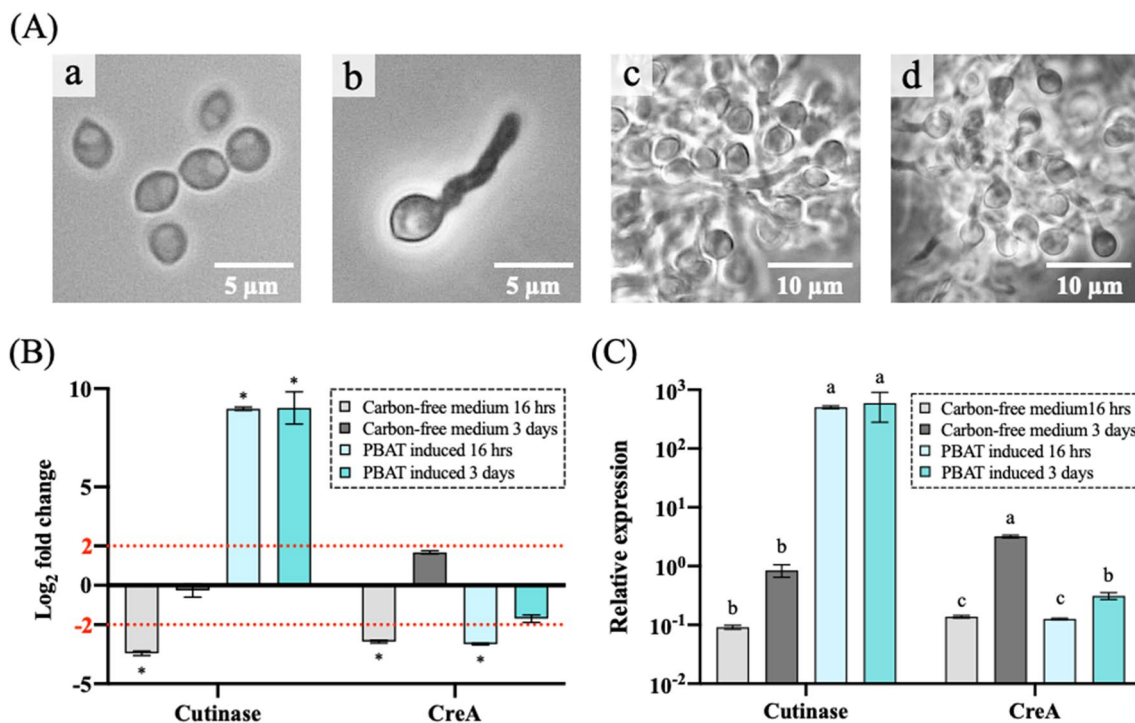


Fig. 6 Gene expression of *P. lilacinum* BA1S in the early stages of culture with PBAT film. The spores were cultured with PBAT films or cultured in carbon-free medium for 16 h and 3 days of incubation, respectively. The gene expression of the ungerminated spores was used as a reference for the analyses. **A** The morphologies of the *P. lilacinum* BA1S spores under optical microscopy: (a) ungerminated spores; (b) germinated spores; (c) germinated spores after culturing in carbon-free medium for 16 h; (d) germinated spores after cultur-

ing with PBAT films for 16 h. **B** Differential expression analyses by qPCR based on log₂-fold change values for *creA* and *cutinase* genes. The dotted line indicates that the value over the threshold of 2 was designated a significant difference (*). The dataset of this plot is provided in Table S2. **C** Relative expression (2^{-ΔΔCT}) values of *creA* and *cutinase* genes were determined by qPCR. The values of each trial were expressed as the mean ± standard deviation ($p < 0.05$; Tukey's post hoc ANOVA)

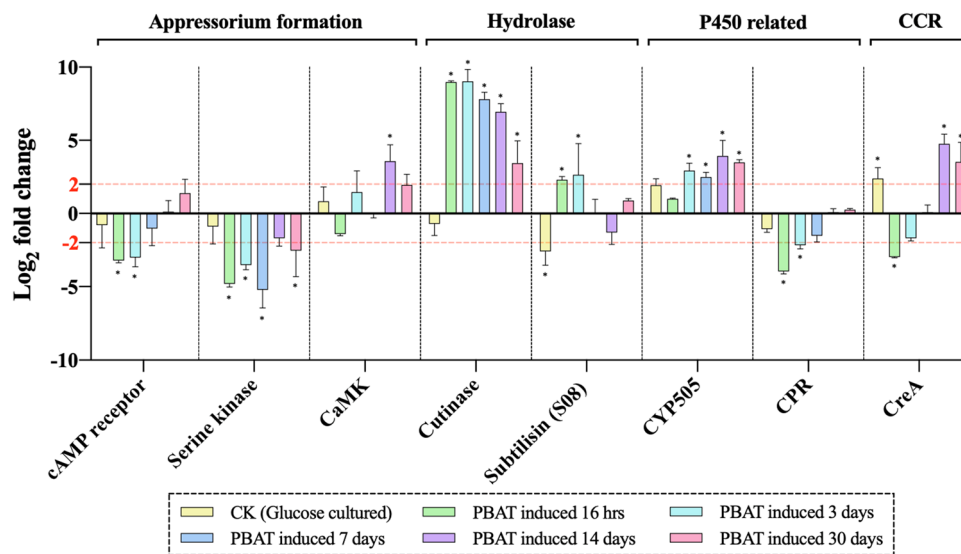


Fig. 7 Gene expression analysis of *P. lilacinum* BA1S induced by PBAT films for long-term incubation (16 h–30 days). The spores were cultured with PBAT films in carbon-free medium for 16 h, 3 days, 7 days, 14 days, and 30 days. The gene expression of the ungerminated spores was used as a reference for the analyses. CK represents the control trial cultured with glucose as the carbon source for 5–7 days. Differential expression analyses by qPCR based on log₂-fold change values for appressorium formation-associated genes (cAMP receptor, serine kinase, Ca²⁺/calmodulin-dependent protein

kinase (CaMK)), hydrolase genes (cutinase and subtilisin (S08)), cytochrome P450-related genes (CYP505 and cytochrome P450 reductase (CPR)), and carbon catabolite repression (CCR)-regulated gene (CreA). The dotted line on the chart indicates that a value over the threshold of 2 was designated as a significant difference (**). The values of the treatments were expressed as the mean \pm standard deviation ($p < 0.05$; Tukey's post hoc ANOVA test). The dataset of this plot is provided in Table S3

incubation; however, the expression of the CCR-regulated gene (CreA) was downregulated in the early stage and significantly upregulated at 14 dpi.

Considering the relative expression level for the above-mentioned genes (Figs. S4A–H), the expression of the appressorium formation-related genes was upregulated after incubation for two weeks (Figs. S4A–C). In addition, we found that the expression levels of the hydrolase genes, especially the cutinase gene, were significantly enhanced in the early stages of PBAT incubation and decreased after 7 days (Figs. S4D and E). In addition, increased expression of cytochrome P450-related genes (CYP505 and CPR) was observed in the later stage of incubation (Figs. S4F and G), and the CreA gene was significantly increased at 14 dpi (Fig. S4H).

Discussion

In this study, we isolated four PBAT-degrading fungal strains from farmlands, and *Purpureocillium lilacinum* strain BA1S showed the highest degradation potential under mesophilic conditions, reaching approximately 15% weight loss within 30 days of incubation (Fig. 2B).

Appressoria, which is a highly specialized adhesion structure of hyphae that uses turgor pressure to punch through the host surface, could be found on BA1S-treated PBAT

films (Fig. 3C), (Chethana et al. 2021; Holland et al. 1999). Appressoria can be used for not only infection but also colonization on hydrophobic inorganic materials and have been observed on starch-plastic films during biodegradation in soils (Lopez-Llorca and Valiente 1993). However, gene expression analysis of appressorium formation-associated genes, including cAMP receptor, serine kinase and Ca²⁺/calmodulin-dependent protein kinase (CaMK) (Fig. 7), showed that there was no difference between the PBAT-treated group and the non-PBAT-treated group. Therefore, we assume that the appressorium formation of BA1S was not significantly induced in the presence of PBAT films and was not directly related to its degradation ability.

In our study, all characteristic peaks in the FTIR spectra decreased after PBAT degradation (Fig. S2), similar to a previous study (Han et al. 2021). The reduced peaks of the ester bond at 1710 cm⁻¹ (i.e., C=O stretching in the ester bond) and 1255 cm⁻¹ (i.e., C-O twisting in the ester bond) suggested that ester bonds underwent hydrolytic cleavage and the PBAT film were degraded (Han et al. 2021; Kijchavengkul et al. 2010a). This result indicated that the PBAT biodegradability of BA1S was related to enzymatic hydrolysis.

Previous studies have indicated that the cutinases of bacteria or fungi, such as *Thermobifida cellulosilytica* DSM44535 (i.e., Thc_Cut1) and *Fusarium solani pisi* (i.e., FsC), could efficiently degrade PBAT (Perz et al. 2016;

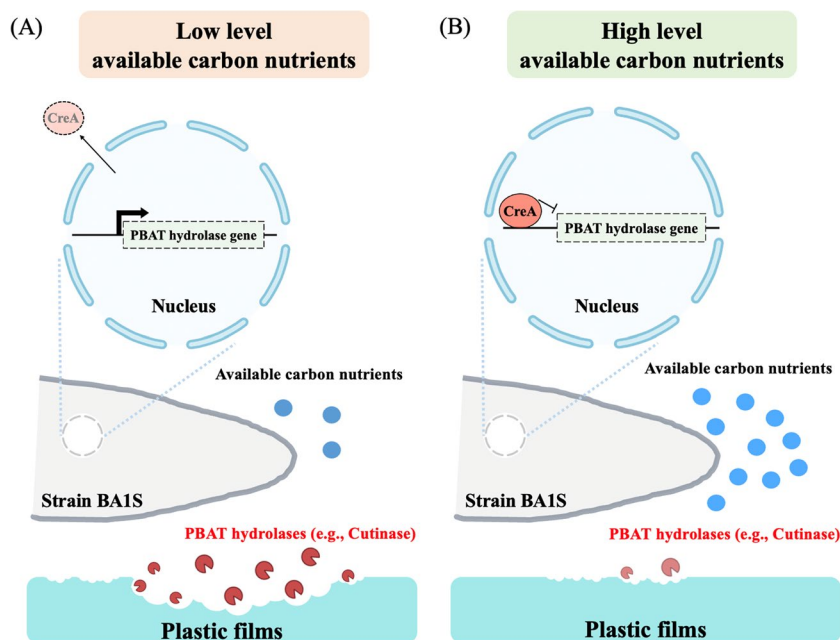
Zumstein et al. 2017). The enzyme is a lipolytic enzyme and acts on short–medium-chain acyl esters up to approximately C8–C10 (Kaushal et al. 2021; Kawai et al. 2019). In our study, the activities of the lipolytic enzymes against the fatty acids of C4, C8, C10, and C12 chain lengths of BA1S were significantly induced when cultured with the PBAT films (Fig. 4), suggesting that the activities were associated with the PBAT-degrading ability of BA1S. Furthermore, the cutinase gene expression of BA1S at different incubation time points was significantly increased in the presence of PBAT films (Fig. S4D). Accordingly, cutinase may play an essential role in the degradation of PBAT by *P. lilacinum* BA1S. However, the catalytic mechanism needs to be elucidated to increase its degradation rate.

Intracellular cytochrome P450 (CYP) monooxygenase activity plays an essential role in plastic degradation (Ali et al. 2021). This enzyme catalyzes the hydroxylation of nonactivated hydrocarbons from lipophilic compounds to more hydrophilic derivatives during the metabolic pathway (Črešnar and Petrič 2011; Isin and Guengerich 2007). We assessed the expression of the related genes (CYP505 and CPR) and the enzyme activities to elucidate their relationship with the biodegradation of PBAT. As shown in Figs. S4F and G, the CYP505 gene [one of the P450 enzymes from the CYP505 family, which can catalyze hydroxylation reactions of n-alkanes and fatty acids (Maseme et al. 2020)] and the cytochrome P450 reductase gene (CPR) were upregulated and significantly increased at the later stage of incubation. In a previous study, Zampolli et al. reported that the transcript of the *cyp450* gene (encoding cytochrome P450 hydroxylase) in a vegetative bacterium, *Rhodococcus opacus* strain R7, was

significantly upregulated in the presence of polyethylene (PE) (Zampolli et al. 2021). Because the expression of each CYP is influenced by a unique combination of mechanisms and factors in each organism, biodegradation of the polyesters (i.e., PBAT, PE, etc.) can trigger similar expression in fungi and bacteria. In this study, we determined the enzymatic activity of NADPH-cytochrome P450 reductase (CPR) to represent the activity of cytochrome P450 as described previously (Jing et al. 2018). As shown in Fig. 5B, the CPR activities induced by the PBAT films from 7–21 days were higher than those of the control. This result is consistent with the transcript result shown in Fig. S4G. In summary, the increased activities of cytochrome P450 and reductase indicated that the elite fungal strain BA1S assimilated alternate carbon sources (i.e., polyesters, such as PBAT) by P450-mediated biodegradation to sustain its growth in carbon-free medium.

However, slow degradation of PBAT occurred after 14 days of incubation (Fig. 2). In addition, the expression level of the cutinase gene began to decrease after 7 days when BA1S was cultured with PBAT films (Figs. S4D and E). Several studies have indicated that carbon catabolite repression (CCR) affects hydrolase production and inhibits polyester degradation. For example, PBAT hydrolase production of *Isaria fumosorosea* NKCM1712 was suppressed while cultivating in glucose/or fructose minimal medium and LB medium (Kasuya et al. 2009). Polyurethane (PU) degradation by *Pseudomonas* sp. was also inhibited during cultivation in glucose minimal medium (Hung et al. 2016). To elucidate the role of CCR in PBAT degradation, we analyzed the gene expression of several hydrolytic enzymes and CreA in strain BA1S. The gene expression of the CreA

Fig. 8 Schematic diagram of hypothetical model of carbon catabolite repression (CCR) regulation on PBAT biodegradation by *P. lilacinum* BA1S. **A** When the available carbon nutrients were insufficient to sustain the growth of BA1S, the PBAT hydrolases (e.g., cutinase) were induced and secreted, resulting in the increase of degradation. **B** When the available carbon nutrients were abundant in the environment, the CreA-mediated CCR inhibited the expression of PBAT hydrolases and resulted in the decrease of degradation. This illustration was created at BioRender.com



gene was initially downregulated at the early stage but significantly upregulated after 14 days of incubation (Fig. 7). We deduced that the downregulation of CreA may be due to carbon starvation when BA1S was cultured with PBAT films in carbon-free medium. The lipolytic enzymes were significantly upregulated in the early stage (Fig. 6), and the degraded PBAT products were utilized as secondary carbon sources as a result. These compounds stimulate the gene expression of CreA, which leads to CCR and causes the inhibition of PBAT degradation in the later stage. This hypothetical CCR regulation mechanism of PBAT degradation by strain BA1S is shown in Fig. 8.

In general, adipic acid (AA), terephthalic acid (TPA), and 1,4-butanediol (BDO) remain at the end of PBAT degradation (Witt et al. 2001). In this study, two TPA (terephthalate) derivatives of PBAT monomers, i.e., $C_8H_6O_4$ (166.03 g/mol) and $C_8H_6O_3^-$ (149.02 g/mol), remained in the culture medium after 14 days of degradation (Fig. S3). Because no AA and BDO monomers were detected, the ester groups in the aliphatic BA section were almost completely degraded. It has been reported that the ester groups in the aliphatic BA section are more susceptible to hydrolysis than those in the aromatic BT sections (Kijchavengkul et al. 2010b). Zumstein et al. found that PBAT degradation is asymmetric and affected by the terephthalate content (Zumstein et al. 2017). TPA usually accumulates in large amounts during the biodegradation of PET or PBAT (Gao et al. 2022; Jia et al. 2021b). There are some microbes that were degraded TPA effectively. For example, *Comamonas* sp. strain E6 and *Arthrobacter* sp. 0574 could utilize TPA as their sole carbon source (Sasoh et al. 2006; Zhang et al. 2013). *Rhodococcus* sp. strain RHA1 and *Pseudomonas umsongensis* GO16 were able to degrade TPA (Hara et al. 2007; Narancic et al. 2021). It has been assumed that the released TPA was further degraded by the microbes via either aromatizing dehydrogenases or cofactor-free decarboxylases (Boll et al. 2020). Accordingly, coinoculating TPA monomer degraders with BA1S or treating with associative enzymes are feasible strategies for degrading PBAT more thoroughly, although they remain to be proven.

P. lilacinum strain BA1S showed a superior PBAT degradation rate, in which lipolytic enzyme activities were induced during coculture with PBAT, and the cutinase gene was significantly upregulated during PBAT degradation. The activity of intracellular cytochrome P450 (CYP) monooxygenase was verified to be correlated with the utilization of PBAT in BA1S cells. CreA-mediated carbon catabolite repression was confirmed to be involved in regulating PBAT-degrading hydrolases and affected the degradation efficiency.

Supplementary Information The online version contains supplementary material available at <https://doi.org/10.1007/s00253-023-12704-z>.

Acknowledgements We thank the Joint Center for Instruments and Researchers, College of Bio-Resources and Agriculture, NTU, for their technical assistance with SEM.

Author contributions WT conceived and conducted most of the experiments, experimental data analysis, and manuscript writing. ML assisted with the experiments. JW provided FTIR and LC/MS analysis services. SC, SH, and SK provided resources and recommendations. CL is the corresponding author in charge of the project design, supervision, and manuscript writing. All authors have read and approved the manuscript.

Funding This study was supported by grants from the Ministry of Science and Technology (MOST 111-2313-B-002-036).

Data availability All data generated in this study are available from the manuscript or the corresponding supplementary material.

Declarations

Ethics approval This article does not contain any studies with human participants or animals performed by any of the authors.

Conflict of interest The authors declare no competing interests.

References

- Ali SS, Elsamahy T, Al-Tohamy R, Zhu D, Mahmoud YA-G, Koutra E, Metwally MA, Kornaros M, Sun J (2021) Plastic wastes biodegradation: mechanisms, challenges and future prospects. *Sci Total Environ* 780:146590. <https://doi.org/10.1016/j.scitotenv.2021.146590>
- Atiq N, Ahmed S, Ali MI, Ahmad B, Robson G (2010) Isolation and identification of polystyrene biodegrading bacteria from soil. *Afr J Microbiol Res* 4(14):1537–1541. <https://doi.org/10.5897/AJMR.9000457>
- Battaglia E, Visser L, Nijssen A, van Veluw G, Wösten H, de Vries R (2011) Analysis of regulation of pentose utilisation in *Aspergillus niger* reveals evolutionary adaptations in *Eurotiales*. *Stud Mycol* 69(1):31–38. <https://doi.org/10.3114/sim.2011.69.03>
- Benguenab A, Chibani A (2021) Biodegradation of petroleum hydrocarbons by filamentous fungi (*Aspergillus ustus* and *Purpureocillium lilacinum*) isolated from used engine oil contaminated soil. *Acta Ecol Sin* 41(5):416–423. <https://doi.org/10.1016/j.chnaes.2020.10.008>
- Boll M, Geiger R, Junghare M, Schink B (2020) Microbial degradation of phthalates: biochemistry and environmental implications. *Environ Microbiol Rep* 12(1):3–15. <https://doi.org/10.1111/1758-2229.12787>
- Bordes P, Pollet E, Avérous L (2009) Nano-biocomposites: biodegradable polyester/nanoclay systems. *Prog Polym Sci* 34(2):125–155. <https://doi.org/10.1016/j.progpolymsci.2008.10.002>
- Buchholz PC, Feuerriegel G, Zhang H, Perez-Garcia P, Nover LL, Chow J, Streit WR, Pleiss J (2022) Plastics degradation by hydrolytic enzymes: The plastics-active enzymes database—PAZy. *Proteins Struct Funct Bioinf* 90(7):1443–1453. <https://doi.org/10.1002/prot.26325>
- Chethana K, Jayawardena RS, Chen Y-J, Konta S, Tibpromma S, Abeywickrama PD, Gomdola D, Balasuriya A, Xu J, Lumyong S (2021) Diversity and Function of Appressoria. *Pathogens* 10(6):746. <https://doi.org/10.3390/pathogens10060746>
- Chien H-L, Tsai Y-T, Tseng W-S, Wu J-A, Kuo S-L, Chang S-L, Huang S-J, Liu C-T (2022) Biodegradation of PBSA Films by Elite


- Aspergillus* Isolates and Farmland Soil. *Polymers* 14(7):1320. <https://doi.org/10.3390/polym14071320>
- Črešnar B, Petrič Š (2011) Cytochrome P450 enzymes in the fungal kingdom. *Biochim Biophys Acta Proteins Proteom* 1814(1):29–35. <https://doi.org/10.1016/j.bbapap.2010.06.020>
- Gao R, Pan H, Kai L, Han K, Lian J (2022) Microbial degradation and valorization of poly (ethylene terephthalate)(PET) monomers. *World J Microbiol Biotechnol* 38(5):1–14. <https://doi.org/10.1007/s11274-022-03270-z>
- Gardes M, Bruns TD (1993) ITS primers with enhanced specificity for basidiomycetes-application to the identification of mycorrhizae and rusts. *Mol Ecol* 2(2):113–118. <https://doi.org/10.1111/j.1365-294X.1993.tb00005.x>
- Gilham D, Lehner R (2005) Techniques to measure lipase and esterase activity in vitro. *Methods* 36(2):139–147. <https://doi.org/10.1016/j.ymeth.2004.11.003>
- Guengerich FP, Martin MV, Sohl CD, Cheng Q (2009) Measurement of cytochrome P450 and NADPH–cytochrome P450 reductase. *Nat Protoc* 4(9):1245–1251. <https://doi.org/10.1038/nprot.2009.121>
- Han Y, Teng Y, Wang X, Ren W, Wang X, Luo Y, Zhang H, Christie P (2021) Soil type driven change in microbial community affects poly (butylene adipate-co-terephthalate) degradation potential. *Environ Sci Technol* 55(8):4648–4657. <https://doi.org/10.1021/acs.est.0c04850>
- Hara H, Eltis LD, Davies JE, Mohn WW (2007) Transcriptomic analysis reveals a bifurcated terephthalate degradation pathway in *Rhodococcus* sp. strain RHA1. *J Bacteriol* 189(5):1641–1647. <https://doi.org/10.1128/JB.01322-06>
- Holland R, Williams K, Khan A (1999) Infection of *Meloidogyne javanica* by *Paecilomyces lilacinus*. *Nematology* 1(2):131–139. <https://doi.org/10.1163/156854199508090>
- Huang Y, Lu X-P, Wang L-L, Wei D, Feng Z-J, Zhang Q, Xiao L-F, Dou W, Wang J-J (2015) Functional characterization of NADPH-cytochrome P450 reductase from *Bactrocera dorsalis*: possible involvement in susceptibility to malathion. *Sci Rep* 5(1):1–12. <https://doi.org/10.1038/srep18394>
- Hung C-S, Zingarelli S, Nadeau LJ, Biffinger JC, Drake CA, Crouch AL, Barlow DE, Russell JN Jr, Crookes-Goodson WJ (2016) Carbon catabolite repression and Impranil polyurethane degradation in *Pseudomonas protegens* strain Pf-5. *Appl Environ Microbiol* 82(20):6080–6090. <https://doi.org/10.1128/AEM.01448-16>
- Hwang B-Y, Kim J-H, Kim J, Kim B-G (2005) Screening of *Exiguobacterium acetylicum* from soil samples showing enantioselective and alkalotolerant esterase activity. *Biotechnol Bioprocess Eng* 10(4):367–371. <https://doi.org/10.1007/BF02931857>
- Isin EM, Guengerich FP (2007) Complex reactions catalyzed by cytochrome P450 enzymes. *Biochim Biophys Acta Gen Subj* 1770(3):314–329. <https://doi.org/10.1016/j.bbagen.2006.07.003>
- Jia H, Zhang M, Weng Y, Li C (2021) Degradation of polylactic acid/polybutylene adipate-co-terephthalate by coculture of *Pseudomonas mendocina* and *Actinomyces elegans*. *J Hazard Mater* 403:123679. <https://doi.org/10.1016/j.jhazmat.2020.123679>
- Jia H, Zhang M, Weng Y, Zhao Y, Li C, Kanwal A (2021b) Degradation of poly (butylene adipate-co-terephthalate) by *Stenotrophomonas* sp. YCJ1 isolated from farmland soil. *J Environ Sci* 103:50–58. <https://doi.org/10.1016/j.jes.2020.10.001>
- Jian J, Xiangbin Z, Xianbo H (2020) An overview on synthesis, properties and applications of poly (butylene-adipate-co-terephthalate)–PBAT. *Adv Ind Eng Polym Res* 3(1):19–26. <https://doi.org/10.1016/j.aiepr.2020.01.001>
- Jing T-X, Tan Y, Ding B-Y, Dou W, Wei D-D, Wang J-J (2018) NADPH–cytochrome P450 reductase mediates the resistance of *Aphis citricidus* (Kirkaldy) to abamectin. *Front Physiol* 9:986. <https://doi.org/10.3389/fphys.2018.00986>
- Kargarzadeh H, Galeski A, Pawlak A (2020) PBAT green composites: Effects of kraft lignin particles on the morphological, thermal, crystalline, macro and micromechanical properties. *Polymer* 203:122748. <https://doi.org/10.1016/j.polymer.2020.122748>
- Kasuya K-i, Ishii N, Inoue Y, Yazawa K, Tagaya T, Yotsumoto T, Kazahaya J-i, Nagai D (2009) Characterization of a mesophilic aliphatic–aromatic copolyester-degrading fungus. *Polym Degrad Stab* 94(8):1190–1196. <https://doi.org/10.1016/j.polymdegradstab.2009.04.013>
- Kaushal J, Khatri M, Arya SK (2021) Recent insight into enzymatic degradation of plastics prevalent in the environment: A mini-review. *Clean Eng Technol* 2:100083. <https://doi.org/10.1016/j.clet.2021.100083>
- Kawai F, Kawabata T, Oda M (2019) Current knowledge on enzymatic PET degradation and its possible application to waste stream management and other fields. *Appl Microbiol Biotechnol* 103(11):4253–4268. <https://doi.org/10.1007/s00253-019-09717-y>
- Kijchavengkul T, Auras R, Rubino M, Alvarado E, Montero JRC, Rosales JM (2010a) Atmospheric and soil degradation of aliphatic–aromatic polyester films. *Polym Degrad Stab* 95(2):99–107. <https://doi.org/10.1016/j.polymdegradstab.2009.11.048>
- Kijchavengkul T, Auras R, Rubino M, Selke S, Ngouajio M, Fernandez RT (2010b) Biodegradation and hydrolysis rate of aliphatic aromatic polyester. *Polym Degrad Stab* 95(12):2641–2647. <https://doi.org/10.1016/j.polymdegradstab.2010.07.018>
- Kilic NT, Can BN, Kodall M, Ozkoc G (2019) Compatibilization of PLA/PBAT blends by using Epoxy-POSS. *J Appl Polym Sci* 136(12):47217. <https://doi.org/10.1002/app.47217>
- Krzan A, Hemjinda S, Miertus S, Corti A, Chiellini E (2006) Standardization and certification in the area of environmentally degradable plastics. *Polym Degrad Stab* 91(12):2819–2833. <https://doi.org/10.1016/j.polymdegradstab.2006.04.034>
- Lee S-Y, Ten LN, Das K, You Y-H, Jung H-Y (2021) Biodegradative activities of fungal strains isolated from terrestrial environments in Korea. *Mycobiology* 49(3):285–293. <https://doi.org/10.1080/12298093.2021.1903131>
- Livak KJ, Schmittgen TD (2001) Analysis of relative gene expression data using real-time quantitative PCR and the 2⁻ΔΔCT method. *Methods* 25(4):402–408. <https://doi.org/10.1006/meth.2001.1262>
- Lopez-Llorca LV, Valiente MFC (1993) Study of biodegradation of starch-plastic films in soil using scanning electron microscopy. *Micron* 24(5):457–463. [https://doi.org/10.1016/0968-4328\(93\)90024-U](https://doi.org/10.1016/0968-4328(93)90024-U)
- Maseme MJ, Pennec A, van Marwijk J, Opperman DJ, Smit MS (2020) CYP505E3: A Novel Self-Sufficient ω-7 In-Chain Hydroxylase. *Angew Chem Int* 132(26):10445–10448. <https://doi.org/10.1002/ange.202001055>
- Matthews S, Belcher JD, Tee KL, Girvan HM, McLean KJ, Rigby SE, Levy CW, Leys D, Parker DA, Blankley RT (2017) Catalytic determinants of alkene production by the cytochrome P450 peroxxygenase OleTJE. *J Biol Chem* 292(12):5128–5143. <https://doi.org/10.1074/jbc.M116.762336>
- Nagarajan V, Misra M, Mohanty AK (2013) New engineered biocomposites from poly (3-hydroxybutyrate-co-3-hydroxyvalerate) (PHBV)/poly (butylene adipate-co-terephthalate)(PBAT) blends and switchgrass: Fabrication and performance evaluation. *Ind Crops Prod* 42:461–468. <https://doi.org/10.1016/j.indcrop.2012.05.042>
- Narancic T, Salvador M, Hughes GM, Beagan N, Abdulmutalib U, Kenny ST, Wu H, Saccomanno M, Um J, O'Connor KE (2021) Genome analysis of the metabolically versatile *Pseudomonas unsongensis* GO16: the genetic basis for PET monomer upcycling into polyhydroxyalkanoates. *Microb Biotechnol* 14(6):2463–2480. <https://doi.org/10.1111/1751-7915.13712>
- Perz V, Bleymaier K, Sinkel C, Kueper U, Bonnekesel M, Ribitsch D, Guebitz GM (2016) Substrate specificities of cutinases on aliphatic–aromatic polyesters and on their model substrates. *N Biotechnol* 33(2):295–304. <https://doi.org/10.1016/j.nbt.2015.11.004>

- Pfaffl MW (2001) A new mathematical model for relative quantification in real-time RT-PCR. *Nucleic Acids Res* 29(9):e45–e45. <https://doi.org/10.1093/nar/29.9.e45>
- Ragonezi C, Caldeira AT, Rosário Martins M, Salvador C, Santos-Silva C, Ganhão E, Klimaszewska K, Zavattieri A (2013) Molecular approach to characterize ectomycorrhizae fungi from Mediterranean pine stands in Portugal. *Braz J Microbiol* 44(2):657–665. <https://doi.org/10.1590/S1517-83822013005000035>
- Rychter P, Kawalec M, Sobota M, Kurcok P, Kowalczyk M (2010) Study of aliphatic-aromatic copolyester degradation in sandy soil and its ecotoxicological impact. *Biomacromol* 11(4):839–847. <https://doi.org/10.1021/bm901331t>
- Saadi Z, Cesar G, Bewa H, Benguigui L (2013) Fungal degradation of poly (butylene adipate-co-terephthalate) in soil and in compost. *J Polym Environ* 21(4):893–901. <https://doi.org/10.1007/s10924-013-0582-2>
- Sarven M, Aminuzzaman F, Huq M (2019) Dose-response relations between *Purpureocillium lilacinum* PLSAU-1 and *Meloidogyne incognita* infecting brinjal plant on plant growth and nematode management: a greenhouse study. *Egypt J Biol Pest Control* 29(1):1–9. <https://doi.org/10.1186/s41938-019-0128-6>
- Sasoh M, Masai E, Ishibashi S, Hara H, Kamimura N, Miyauchi K, Fukuda M (2006) Characterization of the terephthalate degradation genes of *Comamonas* sp. strain E6. *Appl Environ Microbiol* 72(3):1825–1832. <https://doi.org/10.1128/AEM.72.3.1825-1832.2006>
- Sato S, Saika A, Shinozaki Y, Watanabe T, Suzuki K, Sameshima-Yamashita Y, Fukuoka T, Habe H, Morita T, Kitamoto H (2017) Degradation profiles of biodegradable plastic films by biodegradable plastic-degrading enzymes from the yeast *Pseudozyma antarctica* and the fungus *Paraphoma* sp. B47–9. *Polym Degrad Stab* 141:26–32. <https://doi.org/10.1016/j.polyimdegradstab.2017.05.007>
- Šerá J, Stloukal P, Jančová P, Verney V, Pekařová S, Koutný M (2016) Accelerated biodegradation of agriculture film based on aromatic-aliphatic copolyester in soil under mesophilic conditions. *J Agric Food Chem* 64(28):5653–5661. <https://doi.org/10.1021/acs.jafc.6b01786>
- Shah AA, Hasan F, Hameed A, Ahmed S (2008) Biological degradation of plastics: a comprehensive review. *Biotechnol Adv* 26(3):246–265. <https://doi.org/10.1016/j.biotechadv.2007.12.005>
- Spina F, Tummino ML, Poli A, Prigione V, Ilieva V, Cocconcelli P, Puglisi E, Bracco P, Zanetti M, Varese GC (2021) Low density polyethylene degradation by filamentous fungi. *Environ Pollut* 274:116548. <https://doi.org/10.1016/j.envpol.2021.116548>
- Svoboda P, Dvorackova M, Svobodova D (2019) Influence of biodegradation on crystallization of poly (butylene adipate-co-terephthalate). *Polym Adv Technol* 30(3):552–562. <https://doi.org/10.1002/pat.4491>
- Tan FT, Cooper DG, Marić M, Nicell JA (2008) Biodegradation of a synthetic co-polyester by aerobic mesophilic microorganisms. *Polym Degrad Stab* 93(8):1479–1485. <https://doi.org/10.1016/j.polyimdegradstab.2008.05.005>
- Wang G, Liu Z, Lin R, Li E, Mao Z, Ling J, Yang Y, Yin W-B, Xie B (2016) Biosynthesis of antibiotic leucinostatins in bio-control fungus *Purpureocillium lilacinum* and their inhibition on *Phytophthora* revealed by genome mining. *PLoS Pathog* 12(7):e1005685. <https://doi.org/10.1371/journal.ppat.1005685>
- Witt U, Einig T, Yamamoto M, Kleeberg I, Deckwer W-D, Müller R-J (2001) Biodegradation of aliphatic-aromatic copolyesters: evaluation of the final biodegradability and ecotoxicological impact of degradation intermediates. *Chemosphere* 44(2):289–299. [https://doi.org/10.1016/S0045-6535\(00\)00162-4](https://doi.org/10.1016/S0045-6535(00)00162-4)
- Xia M, Bao P, Liu A, Li S, Yu R, Liu Y, Li J, Wu X, Huang C, Chen M (2019) Application of the kinetic and isotherm models for better understanding of the mechanism of biomineralization process induced by *Purpureocillium lilacinum* Y3. *Colloids Surf B Biointerfaces* 181:207–214. <https://doi.org/10.1016/j.colsurfb.2019.05.051>
- Xu J, Cui Z, Nie K, Cao H, Jiang M, Xu H, Tan T, Liu L (2019) A quantum mechanism study of the cc bond cleavage to predict the bio-catalytic polyethylene degradation. *Front Microbiol* 10:489. <https://doi.org/10.3389/fmicb.2019.00489>
- Yamamoto-Tamura K, Hiradate S, Watanabe T, Koitabashi M, Sameshima-Yamashita Y, Yarimizu T, Kitamoto H (2015) Contribution of soil esterase to biodegradation of aliphatic polyester agricultural mulch film in cultivated soils. *AMB Express* 5(1):1–8. <https://doi.org/10.1186/s13568-014-0088-x>
- Yang F, Abdelnabby H, Xiao Y (2015) The role of a phospholipase (PLD) in virulence of *Purpureocillium lilacinum* (*Paecilomyces lilacinum*). *Microb Pathog* 85:11–20. <https://doi.org/10.1016/j.micpath.2015.05.008>
- Yeom S-J, Le T-K, Yun C-H (2021) P450-driven plastic-degrading synthetic bacteria. *Trends Biotechnol*. <https://doi.org/10.1016/j.tibtech.2021.06.003>
- Yoshida S, Hiraga K, Takehana T, Taniguchi I, Yamaji H, Maeda Y, Toyohara K, Miyamoto K, Kimura Y, Oda K (2016) A bacterium that degrades and assimilates poly (ethylene terephthalate). *Science* 351(6278):1196–1199. <https://doi.org/10.1126/science.aad6359>
- Zampolli J, Orro A, Manconi A, Ami D, Natalello A, Di Gennaro P (2021) Transcriptomic analysis of *Rhodococcus opacus* R7 grown on polyethylene by RNA-seq. *Sci Rep* 11(1):1–14. <https://doi.org/10.1038/s41598-021-00525-x>
- Zhang Y-M, Sun Y-Q, Wang Z-J, Zhang J (2013) Degradation of terephthalic acid by a newly isolated strain of *Arthrobacter* sp. 0574. *S Afr J Sci* 109(7):1–4. <https://doi.org/10.1590/sajs.2013/20120019>
- Zumstein MT, Rechsteiner D, Roduner N, Perz V, Ribitsch D, Guebitz GM, Kohler H-PE, McNeill K, Sander M (2017) Enzymatic hydrolysis of polyester thin films at the nanoscale: effects of polyester structure and enzyme active-site accessibility. *Environ Sci Technol* 51(13):7476–7485. <https://doi.org/10.1021/acs.est.7b01330>

Publisher's note Springer Nature remains neutral with regard to jurisdictional claims in published maps and institutional affiliations.

Springer Nature or its licensor (e.g. a society or other partner) holds exclusive rights to this article under a publishing agreement with the author(s) or other rightsholder(s); author self-archiving of the accepted manuscript version of this article is solely governed by the terms of such publishing agreement and applicable law.

Authors and Affiliations

Wei-Sung Tseng¹ · Min-Jia Lee¹ · Jin-An Wu² · Shin-Liang Kuo² · Sheng-Lung Chang² · Shu-Juan Huang² · Chi-Te Liu^{1,3,4} 

✉ Chi-Te Liu
chiteliu@ntu.edu.tw

¹ Institute of Biotechnology, National Taiwan University, R412, No. 81, Chang-Xing St, Taipei 106, Taiwan

² Material and Chemical Research Laboratories, Industrial Technology Research Institute, 321 Kuang Fu Rd., Section 2, Hsinchu, Taiwan

³ Department of Agricultural Chemistry, National Taiwan University No. 1, Sec. Roosevelt Road, Taipei 106, Taiwan

⁴ Agricultural Biotechnology Research Center, Academia Sinica, No.128, Sec.2, Academia Rd., Nankang, Taipei 115, Taiwan